

**STRUCTURAL AND SPECTROSCOPIC STUDIES  
ON NEW PYRENE BASED CHALCONE  
DERIVATIVES AS POTENTIAL SOLAR CELL  
MATERIALS**

**SITI NABILLA ALIYA BINTI MOHD NIZAR**

**UNIVERSITI SAINS MALAYSIA**

**2022**

**STRUCTURAL AND SPECTROSCOPIC STUDIES  
ON NEW PYRENE BASED CHALCONE  
DERIVATIVES AS POTENTIAL SOLAR CELL  
MATERIALS**

by

**SITI NABILLA ALIYA BINTI MOHD NIZAR**

**Thesis submitted in fulfilment of the requirements  
for the degree of  
Master of Science**

**November 2022**

## ACKNOWLEDGEMENT

All praises be to Allah SWT who has given unlimited mercy throughout my journey to complete this master's thesis successfully.

First and foremost, my sincere appreciation goes to my supervisor Dr. Suhana Arshad for her guidance, understanding, patience and most importantly, she has provided positive encouragement and a warm spirit for me to finish this master. I am greatly indebted and appreciate her valuable time for guiding and helping me in spite of her busy schedule. My humble gratitude also goes to my co-supervisors, Prof. Dr. Abdul Razak Ibrahim and Dr. Siti Azrah Mohamad Samsuri for the aspiring guidance and support in completing my study. My sincere thanks also to Dr. Dian Alwani Zainuri for giving me encouragement and insightful comments to finish this thesis. Besides, I would like to thank Prof. Madya Dr. Yam Fong Kwong for providing the facilities at Engineering Lab, School of Physics, USM to carry out the Cyclic Voltammetry experiments.

My deepest gratitude goes to all my family members especially my parents, Mr. Mohd Nizar and Mrs. Rohimah, also my grandmother, Mrs. Kamariah for all the prayers, encouragement and sacrifices through my thick and thin journey since I was born. To all my dearest brother and sisters, a big thank you for their support, inspiration and for putting colours in my life, may Allah always bless you all.

Also, I would like to dedicate my appreciation to my partner, Mr. Che Ku Ahmad Luqman for motivating and supporting me throughout my master. Thank you for being a part of my journey and persuade me to never give up through this challenging journey.

I thankfully acknowledge the support and inspiration that I received from my fellow labmates and friends, Ms. Farhana, Ms. Farah, Ms. Rineswary, Ms. Wong Qin Ai, Mr. Amin, Mr. Saleh and Mr. Aizat who never hesitate in sharing the ideas and helping me in my research study. I would like to deliver my special thanks to all X-ray Crystallography laboratory staff, Mr. Mustaqim Rosli, Mr. Mustaqim Abu Bakar and Mr. Aswafi for their assistance and guidance in completing my master project. My special appreciation also to Mrs. Ainizatul for her assistance and suggestions especially during my early stage of master study.

Apart from that, I want to thank the Malaysian government and the Universiti Sains Malaysia for funding my studies through the Research University Grant (No: 1001.PFIZIK.8011115). My gratitude also to MARA for supporting my tuition fee during my study.

Last but not least, I wish to express my sincere thanks to all those who have one way or another helped me in making this study a success. Thank you so much!

## TABLE OF CONTENTS

<b>ACKNOWLEDGEMENT</b> .....	<b>ii</b>
<b>TABLE OF CONTENTS</b> .....	<b>iv</b>
<b>LIST OF TABLES</b> .....	<b>vii</b>
<b>LIST OF FIGURES</b> .....	<b>viii</b>
<b>LIST OF PLATES</b> .....	<b>xii</b>
<b>LIST OF ABBREVIATIONS</b> .....	<b>xiii</b>
<b>LIST OF APPENDICES</b> .....	<b>xv</b>
<b>ABSTRAK</b> .....	<b>xvi</b>
<b>ABSTRACT</b> .....	<b>xviii</b>
<b>CHAPTER 1 INTRODUCTION</b> .....	<b>1</b>
1.1 The Organic Compound of Pyrenyl Chalcone ( <b>PnCh</b> ) Derivatives .....	1
1.2 The Push-pull System of <b>PnCh</b> Derivative .....	3
1.3 The $\pi$ -conjugated <b>PnCh</b> System as Dye-Sensitizer .....	6
1.4 Problem Statement .....	9
1.5 Objectives .....	11
<b>CHAPTER 2 LITERATURE REVIEW</b> .....	<b>12</b>
2.1 The D- $\pi$ -A System of Chalcone Derivative.....	12
2.1.1 D- $\pi$ -A configuration influence the red-shift in the absorption band.....	13
2.1.2 Enhancement of electron injection process in D- $\pi$ -A system .....	14
2.1.3 D- $\pi$ -A configuration induce the planarity backbone .....	14
2.1.4 Improvement of DSSC efficiency in D- $\pi$ -A configuration.....	15
2.2 The Synthetic Process of Pyrenyl Chalcone ( <b>PnCh</b> ) .....	16
2.3 Fourier Transform Infrared (FTIR) Studies .....	17
2.4 Nuclear Magnetic Resonance (NMR) Studies .....	19

2.5	X-Ray Crystallography: Molecular and Crystal Packing Studies.....	22
2.5.1	Molecular Structure of <b>PnCh</b> .....	22
2.5.2	Crystal Packing Analysis.....	25
2.6	UV-Visible (UV-Vis) Spectroscopy.....	27
2.7	Electrochemical studies: Cyclic Voltammetry (CV).....	30
2.8	Dye-sensitized Solar Cell (DSSC) Materials.....	32
2.8.1	Field-Emission Scanning Electron Microscopy (FESEM) and Energy Dispersive X-ray (EDX) Studies.....	32
2.8.2	Solar Cell Performance Studies.....	34
<b>CHAPTER 3 THEORY AND METHODOLOGY.....</b>		<b>37</b>
3.1	The Synthesis and Preparation of Pyrenyl Chalcone ( <b>PnCh</b> ).....	38
3.2	Fourier Transform Infrared Spectroscopy (FTIR) Analysis.....	40
3.2.1	FTIR Characterization and Instrumentation.....	42
3.3	Nuclear Magnetic Resonance (NMR) Studies.....	42
3.3.1	Sample Preparation and Instrumentation.....	44
3.4	Single Crystals X-Ray Crystallography.....	45
3.4.1	Crystal Structure Determination and Crystallographic Software.....	46
3.4.2	X-Ray Crystallography Equipment.....	47
3.5	Ultraviolet-Visible (UV-Vis) Studies.....	48
3.5.1	Sample Preparation, Instrumentation and Software.....	49
3.6	Cyclic Voltammetry (CV) Analysis.....	50
3.6.1	Sample preparation of Cyclic Voltammetry.....	52
3.6.2	Cyclic Voltammetry Instrumentation.....	53
3.7	Solar Cell Applications.....	54
3.7.1	Dye-Synthesized Solar Cell (DSSC) Fabrication.....	55
3.7.2	Characterization and Performance Study of DSSC.....	57
3.7.3	Instrumentation of DSSC Study.....	58

<b>CHAPTER 4</b>	<b>RESULT AND DISCUSSION .....</b>	<b>60</b>
4.1	Fourier Transform Infrared (FTIR) Spectroscopy Studies .....	61
4.2	Nuclear Magnetic Resonance (NMR) Spectroscopy Analysis .....	65
4.3	Molecular and Crystal Structure Analyses .....	69
4.3.1	Molecular Structure Analysis .....	71
4.3.2	Crystal Packing Analysis.....	77
4.4	Ultraviolet-Visible (UV-Vis) Spectroscopy .....	83
4.5	Cyclic Voltammetry (CV) Studies .....	91
4.6	Solar Cell Studies .....	94
4.6.1	Surface Morphology and Elemental Analyses .....	94
4.6.2	Performance Study of Solar Cell .....	100
<b>CHAPTER 5</b>	<b>CONCLUSION AND FUTURE RECOMMENDATIONS ....</b>	<b>106</b>
5.1	Conclusion .....	106
5.2	Future Recommendations .....	108
<b>REFERENCES</b>	<b>.....</b>	<b>109</b>
<b>APPENDICES</b>		
<b>LIST OF PUBLICATIONS</b>		

## LIST OF TABLES

	<b>Page</b>
Table 1.1	Summary of the physical properties of pyrene..... 2
Table 2.1	Assignments of vibrational frequencies value for previously reported <b>PnCh</b> . .... 18
Table 2.2	<sup>1</sup> H isotropic chemical shifts (ppm). .... 20
Table 2.3	<sup>13</sup> C isotropic chemical shifts (ppm). .... 21
Table 2.4	The summary of parameters from redox potentials (Karuppusamy <i>et al.</i> , 2017)..... 31
Table 2.5	The summary of the photovoltaic parameters of the compounds (Anizaim <i>et al.</i> , 2020; Nizar <i>et al.</i> , 2021). .... 36
Table 3.1	Major programs in SHELXTL software. .... 47
Table 4.1	Assignment of vibrational frequencies for difference functional groups in <b>PnCh</b> . .... 62
Table 4.2	<sup>1</sup> H isotropic chemical shifts (ppm). .... 67
Table 4.3	<sup>13</sup> C isotropic chemical shifts (ppm). .... 69
Table 4.4	Crystal data and structure refinement ..... 70
Table 4.5	The selected experimental bond length, bond angle and torsion angle of compounds of <b>PnCh</b> . .... 73
Table 4.6	Dihedral angles of <b>PnCh</b> between the selected planes..... 73
Table 4.7	Hydrogen bond geometry of <b>PnCh</b> . .... 77
Table 4.8	UV-Vis absorbance spectrum of the synthesised <b>PnCh</b> . .... 83
Table 4.9	Cyclic voltammetry parameters..... 92
Table 4.10	The percentage weight of elements in TiO <sub>2</sub> and <b>PnCh</b> . .... 96
Table 4.11	Solar cell parameters and performance of <b>PnCh</b> . .... 102



## LIST OF FIGURES

	<b>Page</b>
Figure 1.1	The Claisen-Schmidt condensation reaction..... 1
Figure 1.2	The molecular structure of pyrene with sixteen number of carbons atoms..... 2
Figure 1.3	A schematic diagram of Type 1 and Type 2 <b>PnCh</b> derivatives. .... 3
Figure 1.4	(a) Push-pull configuration of chalcone derivative (Teo <i>et al.</i> , 2017); the structure of <b>PnCh</b> with (b) D- $\pi$ -conjugated-D and (c) D- $\pi$ -conjugated-A types push-pull effect in the chalcone system (Karuppusamy & Kannan, 2020; Niu <i>et al.</i> , 2020)..... 4
Figure 1.5	UV-Vis spectrum of D- $\pi$ -A and D- $\pi$ -D chalcone derivative (Anizaim <i>et al.</i> , 2021). .... 5
Figure 1.6	Crystal packing showing (a) head-to-tail and (b) head-to-head orientations of intermolecular interaction between the molecules (Alsaeed <i>et al.</i> , 2022; Zaini <i>et al.</i> , 2018). .... 6
Figure 1.7	The 1 <sup>st</sup> , 2 <sup>nd</sup> , and 3 <sup>rd</sup> generation of solar cell evolutions (Olivia-Chatelain & Barron, 2011). .... 7
Figure 1.8	(a) The basic operation of DSSC in structure layered, DSSC performance of (b) organometallic-containing sensitizer and (c) organic-containing sensitizer (Anizaim <i>et al.</i> , 2021; Nizar <i>et al.</i> , 2021). .... 8
Figure 1.9	The <i>J-V</i> curve of the previously reported compounds (Rajakumar <i>et al.</i> , 2012)..... 9
Figure 2.1	Schematic representation of D- $\pi$ -A system featuring ICT (Kulhanek & Bures, 2012). .... 12
Figure 2.2	Absorption spectra of <b>PnCh</b> showing D- $\pi$ -A and D- $\pi$ -D architecture (Karuppusamy <i>et al.</i> , 2022)..... 13

Figure 2.3	Energy level diagram of chalcone derivative with D- $\pi$ -A system (Ibrahim <i>et al.</i> , 2022). ....	14
Figure 2.4	The dihedral angle between two planes for (a) D- $\pi$ -A and (b) D- $\pi$ -D architecture (Zaini <i>et al.</i> , 2020; Anizaim <i>et al.</i> , 2021).....	15
Figure 2.5	<i>J-V</i> curves for DSSCs based on D- $\pi$ -A and D- $\pi$ -D architecture (Anizaim <i>et al.</i> , 2021). ....	16
Figure 2.6	The synthesis scheme of <b>PnCh</b> derivative (Zainuri <i>et al.</i> , 2018b)...	17
Figure 2.7	The vibrational modes studied in chalcone derivatives. ....	18
Figure 2.8	The FTIR spectrum of <b>PnCh</b> compound (Alsaee <i>et al.</i> , 2022). ....	19
Figure 2.9	The <sup>1</sup> H NMR spectrum of <b>PnCh</b> (Atahan, 2021).....	20
Figure 2.10	The <sup>13</sup> C NMR spectrum showing C=O, C <sub><math>\alpha</math></sub> and C <sub><math>\beta</math></sub> in <b>PnCh</b> (D'Aléo <i>et al.</i> , 2015).....	21
Figure 2.11	The molecular structure of core <b>PnCh</b> (Wang <i>et al.</i> , 2008). ....	22
Figure 2.12	The <i>cis</i> , <i>trans</i> , <i>s-cis</i> and <i>s-trans</i> configurations in chalcone. ....	23
Figure 2.13	<b>PnCh</b> with <i>s-trans</i> and <i>trans</i> configurations (Du <i>et al.</i> , 2017). ....	23
Figure 2.14	The <i>s-cis</i> configuration of <b>PnCh</b> (Sun <i>et al.</i> , 2012). ....	24
Figure 2.15	The small dihedral angle of <b>PnCh</b> (a) without and (b) with the presence of methoxy substituents (Che & Perepichka, 2020). ....	24
Figure 2.16	The crystal packing analysis of chalcone derivative showing side-by-side arrangement (Rodriguez-lugo <i>et al.</i> , 2015).....	25
Figure 2.17	Crystal packing of <b>PnCh</b> with head-to-head configurations (Zainuri <i>et al.</i> , 2018a). ....	26
Figure 2.18	Crystal packing of <b>PnCh</b> with head-to-tail configurations shows in green colours (Alsaee <i>et al.</i> , 2022). ....	26
Figure 2.19	UV-Vis spectrum of ( <i>E</i> )-chalcone (Jumina <i>et al.</i> , 2019). ....	27
Figure 2.20	The absorbance spectra of pyrene core (Telitel <i>et al.</i> , 2013). ....	28
Figure 2.21	The absorption spectrum of <b>PnCh</b> (D'Aléo <i>et al.</i> , 2015). ....	29
Figure 2.22	The absorption spectra of substituted <b>PnCh</b> (Alsaee <i>et al.</i> , 2022)....	29

Figure 2.23	Cyclic voltammograms of <b>PnCh</b> with different attachment to the enone bridge (Karuppusamy <i>et al.</i> , 2017).....	31
Figure 2.24	The energy diagram of the reported compounds in the preferable range of HOMO and LUMO calculated from redox potentials (Selvam & Subramanian, 2017). .....	32
Figure 2.25	(a) The FESEM image and (b) EDX spectra of dye sensitized TiO <sub>2</sub> layer (Ghann <i>et al.</i> , 2017). .....	33
Figure 2.26	(a) FESEM image and (b) EDX spectra of previously reported chalcone derivative (Singh <i>et al.</i> , 2022). .....	34
Figure 2.27	The <i>J–V</i> curve for the pyrene-containing compounds (Rajakumar <i>et al.</i> , 2012; Li <i>et al.</i> , 2014a).....	35
Figure 2.28	The <i>J–V</i> curve for the compound a) with and b) without methoxy group attachment (Anizaim <i>et al.</i> , 2020; Nizar <i>et al.</i> , 2021). .....	35
Figure 3.1	The methodology outline of the study. ....	37
Figure 3.2	The synthesis of <b>PnCh</b> derivative. ....	39
Figure 3.3	The overlay of FTIR spectrum (Nandiyanto <i>et al.</i> , 2019). ....	41
Figure 3.4	The effect of IR radiation on the bond molecule (Mendes & Duarte, 2021) .....	41
Figure 3.5	NMR chemical shift for (a) <sup>1</sup> H and (b) <sup>13</sup> C (Gunawan <i>et al.</i> , 2021). .....	43
Figure 3.6	(a) Bragg's law diffraction (Pederson, 2019) and (b) X-ray crystallography principle (Gumustas <i>et al.</i> , 2017). .....	45
Figure 3.7	Crystal structure determination procedure. ....	46
Figure 3.8	Schematic demonstration of electronic transition. (Tourlomousis, 2019). ....	49
Figure 3.9	Cyclic voltammetry set up (Elgrishi <i>et al.</i> , 2018).....	51
Figure 3.10	(a) Excitation signal of cyclic voltammograms and (b) voltammogram of the oxidation-reduction process (Elgrishi <i>et al.</i> , 2018). ....	52

Figure 3.11	The preparation of TiO <sub>2</sub> on glass.....	52
Figure 3.12	Schematic illustration of DSSC (Roslan <i>et al.</i> , 2018). .....	55
Figure 3.13	Illustrative diagram of the DSSC components.....	56
Figure 3.14	The characterization and performance study of DSSC.....	57
Figure 4.1	The FTIR spectra of compound <b>16</b> .....	61
Figure 4.2	(a) <sup>1</sup> H and (b) <sup>13</sup> C NMR spectra of compound <b>16</b> .....	66
Figure 4.3	The molecular structure of studied <b>PnCh</b> .....	72
Figure 4.4	Dihedral angle between pyrene moiety and enone bridge of <b>PnCh</b> . .....	76
Figure 4.5	The crystal packing analysis of compound <b>1</b> showing the C— H···O interactions connects the molecules in head-to-head arrangement.....	78
Figure 4.6	The crystal packing show π—π interactions involving Cg2 and Cg5 in compound <b>9</b> .....	79
Figure 4.7	Packing diagram showing (a) C—H···O and (b) π—π interactions in compound <b>10</b> .....	80
Figure 4.8	The packing of compound <b>11</b> showing C—H···O and C—H··· π interactions forming a chain along the <i>bc</i> -plane direction.....	81
Figure 4.9	A view showing C—H···O interaction propagating along the <i>b</i> -axis in compound <b>12</b> .....	82
Figure 4.10	Ring A and Ring B of Type 1 and Type 2 <b>PnCh</b> derivative, respectively.....	83
Figure 4.11	HOMO and LUMO energy levels of <b>PnCh</b> .....	94
Figure 4.12	Surface morphology of TiO <sub>2</sub> and <b>PnCh (1-18)</b> with FESEM magnifications of x5 000.....	95

## LIST OF PLATES

	<b>Page</b>
Plate 3.1	(a) The PerkinElmer GX Frontier Spectrophotometer utilized for FTIR-ATR spectroscopy and (b) FTIR data analysed using PerkinElmer Spectrum software..... 42
Plate 3.2	Tube used for NMR. .... 44
Plate 3.3	(a) Bruker 500 and 125 MHz Avance III spectrometer for $^1\text{H}$ and $^{13}\text{C}$ NMR, respectively and (b) NMR data analysis using Bruker TOPSPIN 2.1 software..... 44
Plate 3.4	Bruker APEX II Duo CCD Detector Single Crystal X-Ray Diffractometer for data collection. .... 48
Plate 3.5	(a) Volumetric flasks and (b) cuvette containing <b>PnCh</b> derivative for UV-vis characterization, (c) UV-Visible Spectrophotometer Model Cary 5000 UV-Vis-NIR and (d) Origin 8.5 software. .... 50
Plate 3.6	Cyclic voltammetry set up showing (a) Platinum (Pt) as counter electrode, (b) reference electrode, and (c) sample as working electrode. .... 53
Plate 3.7	(a) Nabertherm furnace at Nano-Optoelectronics Research & Laboratory (NOR Lab) and (b) Gamry Interface 1000 Potentiostat located at Engineering Lab, School of Physics, USM. .... 54
Plate 3.8	(a) FEI Nova NanoSEM 450 scanning electron microscope and (b) Computers used for FESEM and EDX analysis, and (c) Keithley 2400 solar simulator..... 59

## LIST OF ABBREVIATIONS

A	Acceptor
ATR	Attenuated Total Reflectance
Ba(OH) <sub>2</sub>	Barium Hydroxide
CCD	Charge-Coupled Device
CCDC	The Cambridge Crystallographic Data Centre
CH <sub>3</sub> OH	Methanol
CIF	Crystallographic Information File
CV	Cyclic Voltammetry
D	Donor
DMSO	Dimethyl Sulfoxide
DSSC	Dye-sensitized Solar Cell
EDG	Electron donating group
EWG	Electron-withdrawing group
FTIR	Fourier Transform Infrared
HOMO	Highest Occupied molecular Orbital
ICT	Intramolecular Charge Transfer
KBr	Potassium Bromide
KOH	Potassium Hydroxide
LiOH	Lithium Hydroxide
LUMO	Lowest Unoccupied Molecular Orbital
NaOH	Sodium Hydroxide
NMR	Nuclear Magnetic Resonance
ORTEP	Oak Ridge Thermal Ellipsoid Plot
ppm	Parts per million

PnCh	Pyrenyl Chalcone
SADABS	Siemens Area Detector Absorption Correction
SAINT	SAX Area-detector Integration (SAX-Siemens Analytical Xray)
SCXRD	Single crystal X-ray diffraction
SOCl <sub>2</sub>	Thionyl Chloride
TMS	Tetramethylsilane
USM	Universiti Sains Malaysia
UV	Ultraviolet
UV-Vis	Ultraviolet Visible

## LIST OF APPENDICES

- Appendix A List of aldehydes (**1-8**) and ketones (**9-18**) derivatives
- Appendix B Precipitate of the synthesized compounds
- Appendix C The front and back view of DSSC component for (a) counter electrode and (b) photoanode, and (c) the electrolyte
- Appendix D FTIR spectra of all compounds
- Appendix E  $^1\text{H}$  and  $^{13}\text{C}$  NMR spectra of all compounds
- Appendix F Cyclic voltammograms of all compounds
- Appendix G Spectroscopic analysis of the synthesized compounds



# KAJIAN STRUKTUR DAN SPEKTROSKOPIK TERBITAN KALKON BERASASKAN PIREN DAN POTENSI SEBAGAI BAHAN SEL SURIA

## ABSTRAK

Satu siri kalkon piren (**PnCh**) telah disintesis secara strategik untuk digunakan di dalam aplikasi sel suria peka pewarna (DSSC) dengan menggunakan kumpulan pengganti penderma dan penerima elektron yang berbeza. Kesemua sebatian telah berjaya disintesis menggunakan kaedah pemewapan Claisen-Schmidt dan menghasilkan 5 hablur tunggal melalui kaedah penyejatan perlahan. Sebatian tersebut seterusnya dicirikan dengan menggunakan spektroskopi FTIR dan NMR untuk mengetahui kehadiran kumpulan berfungsi dan bilangan karbon dan proton di dalam struktur molekul, setiap satunya. Kesemua 5 hablur tunggal yang terbentuk seterusnya dikaji menggunakan analisis pembelauan sinar-X (XRD) dan struktur molekul tiga-dimensi bagi setiap sebatian telah diperiksa. Kehadiran interaksi antara molekul (C-H $\cdots$ O, C-H $\cdots$  $\pi$  dan  $\pi\cdots\pi$ ) dalam padatan hablur telah ditemukan untuk menstabilkan struktur hablur dan meningkatkan pemindahan caj di antara molekul. Analisis UV-Vis telah dijalankan menggunakan pelarut asetonitril untuk mendapatkan nilai jurang tenaga sebatian yang disintesis iaitu dalam julat yang sesuai untuk digunakan sebagai bahan peka pewarna dalam DSSC (2.80-3.06 eV). Tambahan pula, sifat redoks bagi sebatian **PnCh** telah berjaya dipelajari dengan menjalankan analisis CV. Sebatian tersebut terletak pada tahap tenaga HOMO dan LUMO yang sepatutnya di mana mengesahkan kesesuaiannya sebagai bahan peka pewarna. Kemudian, semua sebatian diteruskan untuk kajian prestasi sel suria. Pembuatan lapisan DSSC dicirikan menggunakan analisis FESEM dan EDX untuk mengkaji komposisi morfologi permukaan dan unsur sebatian pada lapisan TiO<sub>2</sub>, setiap satunya. Kumpulan pengganti

yang melekat pada sebatian **PnCh** menunjukkan peningkatan kepada prestasi DSSC yang bertindak sebagai peka pewarna yang baik untuk aplikasi sel suria pada masa hadapan.

**STRUCTURAL AND SPECTROSCOPIC STUDIES ON NEW PYRENE  
BASED CHALCONE DERIVATIVES AS POTENTIAL SOLAR CELL  
MATERIALS**

**ABSTRACT**

A series of Pyrenyl Chalcone (**PnCh**) derivatives have been strategically synthesized for the dye-sensitized solar cell (DSSC) application by proposing different electron donor and acceptor substituent groups. All compounds were successfully synthesized using the Claisen-Schmidt condensation reaction and attained 5 single crystals *via* slow evaporation method. The compounds are characterized using FTIR and NMR spectroscopy to investigate the presence of functional groups and the number of carbons and protons in the molecular structure, respectively. All 5 single crystals obtained are further investigated by X-ray diffraction (XRD) analysis and the three-dimensional molecular structure of each compound is examined. The existence of intermolecular interactions (C-H $\cdots$ O, C-H $\cdots$  $\pi$  and  $\pi\cdots\pi$ ) in the crystal packing are found to stabilize the crystal structure and enhance the charge transfer within the molecules. The UV-Vis analysis has been conducted in acetonitrile solvent to obtain the energy gap value of the synthesized compounds which are particularly in the suitable range as photosensitizer materials in DSSC (2.80 - 3.06 eV). Furthermore, the redox properties of **PnCh** compounds have been successfully studied by conducting CV analysis. The proposed compounds are situated in the appropriate energy levels of HOMO and LUMO which confirms their suitability as dye-sensitizer materials. Then, all compounds are proceeded for solar cell performance studies. The fabrication of the DSSC layers is characterized *via* FESEM and EDX analyses to study the surface morphological and elemental composition of the compound on the TiO<sub>2</sub> layer,

respectively. The substituent groups attached to the **PnCh** compounds show the improvement to the performance of the DSSC which act as excellent photosensitizer for future solar cell application.

## CHAPTER 1

### INTRODUCTION

#### 1.1 The Organic Compound of Pyrenyl Chalcone (PnCh) Derivatives

Chalcone is categorized as a class of aromatic ketones with two aromatic groups connected by the enone linkage (Nizar *et al.*, 2021). Preparation of chalcone involves the Claisen-Schmidt condensation reaction between benzaldehyde and acetophenone with an addition of sodium hydroxide as a catalyst (Figure 1.1).

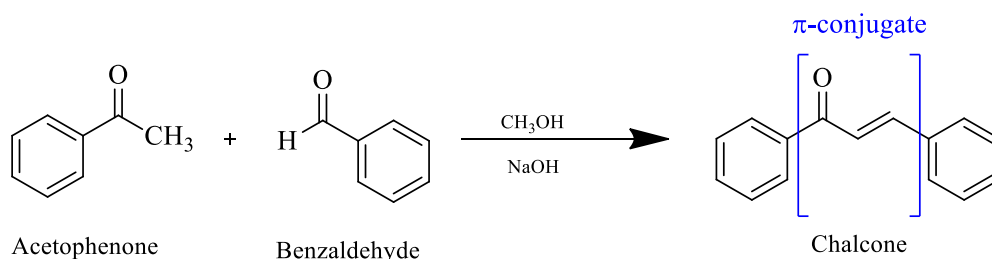


Figure 1.1 The Claisen-Schmidt condensation reaction.

During the past few years, chalcone which is also recognized as 1,3-diarylprop-2-en-1-one framework has been used as a main component for numerous natural products since it is rich in edible plants, also acts as a precursor of flavanoids and isoflavanoids (Kumar *et al.*, 2015). Chalcones are constructed by a planar  $\pi$ -conjugated system (Figure 1.1). The  $\pi$ -conjugation in chalcone refers to the system with an alternation of single and double bonds along the carbon atoms chain (Milián-Medina & Gierschner, 2012). According to Shkir *et al.*, (2015), the existence of  $\pi$ -conjugated systems is able to promote the charge transfer configuration throughout the compound. Herein, the study regarding  $\pi$ -conjugated chalcones is widely explored in various industries such as light-emitting diodes (OLED), dye-sensitized solar cells (DSSC) and non-linear optics (NLO) applications (Anizaim *et al.*, 2021).

Pyrene is a polycyclic aromatic hydrocarbon with four fused benzene rings (Figure 1.2). The structure of pyrene is constructed by sixteen number of carbon atoms, forming planar ring with wide-ranging  $\pi$ -delocalization. The planar configuration of pyrene contributes to the flat  $\pi$ -conjugation structure inducing the fluency result in the flow of electron for outstanding photoelectric effects (Liu *et al.*, 2021). Thus, this led to a good charge transfer property among the electron-donor (D) and acceptor (A) of the  $\pi$ -conjugated pyrenyl derivative.

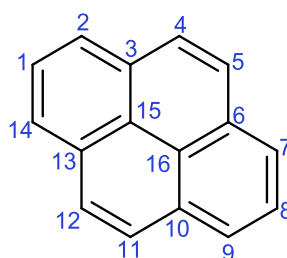


Figure 1.2 The molecular structure of pyrene with sixteen number of carbons atoms.

Pyrene has been widely used as the material in the applications of optical limiting, organic light-emitting diodes (OLEDs) and solar cells due to its physical properties (Islam *et al.*, 2019). The summarization of the physical properties of pyrene are tabulated in Table 1.1.

Table 1.1 Summary of the physical properties of pyrene.

<b>Chemical formula</b>	C <sub>16</sub> H <sub>10</sub>
<b>Molecular weight</b>	202.25 g/mol
<b>Colour</b>	White to Light Yellow
<b>Appearance</b>	Powder or Crystals
<b>Melting point</b>	151 - 154 °C
<b>UV wavelength (Ethanol solvent)</b>	334 - 335 nm

**PnCh** is a chalcone family with both four fused benzene rings and aromatic unit linked by the  $\alpha, \beta$ -unsaturated ketone linkage. Karuppusamy *et al.*, (2017) reported that the existence of pyrene in **PnCh** derivative behave as an electron donor with the locality of substitution in the chalcone unit forming Type 1 or Type 2 derivatives (Figure 1.3). According to the previous research, **PnCh** derivative showing a good property as the electron donating group (EDG) attributes to the high energy  $\pi-\pi^*$  transitions at the range of 320–400 nm (Rajakumar *et al.*, 2011). Additionally, the combination of pyrenyl derivative with an appropriate selection of the donor (-Me, -OMe, -OH, -NH<sub>2</sub> and -S) and acceptor (-F, -Cl, -Br, -CN and -NO<sub>2</sub>) group may lead to the effective configuration of electron transfer throughout the compound (Mori *et al.*, 2016).

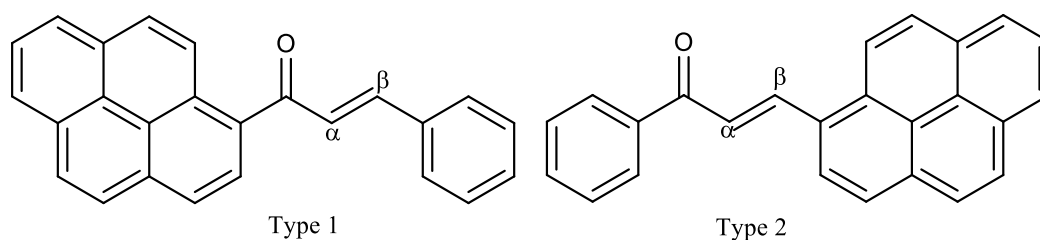


Figure 1.3 A schematic diagram of Type 1 and Type 2 **PnCh** derivatives.

## 1.2 The Push-pull System of PnCh Derivative

Chalcone is an organic class molecule exhibits a push-pull property as shown in Figure 1.4a. The push-pull system is a desire property in delivering a structure with a good intramolecular charge transfer (ICT) within the compound. Therefore, the push-pull system can be created by alternating the donor (D) and acceptor (A) anchoring part of the compound since it leads to the different properties and results (Zainuri *et al.*, 2021). Pyrene are involved in EDG since it donates electrons away from the reaction center when forming a structure. Hence, pyrene functions as an electron donor in the pyrene-based chalcone building. As exemplify in Figure 1.4b and Figure 1.4c,

the previous research on **PnCh** have proposed a structure with D- $\pi$ -conjugated-D and D- $\pi$ -conjugated-A configuration demonstrating a push-pull effect in the chalcone system, respectively (Niu *et al.*, 2020). A strong push-pull effect may arise due to the involvement of electron-rich substituents leading to the increase in the dipole moment result (Ulrich *et al.*, 2014; Zainuri *et al.*, 2021). In addition, a good achievement in push-pull design contribute to the satisfying nonlinear response and photovoltaic conversion (Zainuri *et al.*, 2018a; Anizaim *et al.*, 2020).

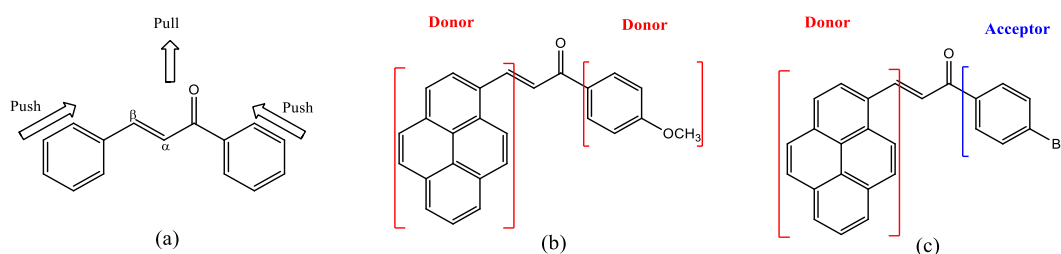


Figure 1.4 (a) Push-pull configuration of chalcone derivative (Teo *et al.*, 2017); the structure of **PnCh** with (b) D- $\pi$ -conjugated-D and (c) D- $\pi$ -conjugated-A types push-pull effect in the chalcone system (Karuppusamy & Kannan, 2020; Niu *et al.*, 2020).

The prior study conducted by Bureš (2014) explained a good transmission of ICT contribute to the strong and bathochromic shift of longest absorption maxima wavelength in the UV-Vis absorption spectra. The chalcone exhibits the D- $\pi$ -A and D- $\pi$ -D configuration showing the strong cut-off wavelength in the UV-Vis spectrum which leading to the small experimental energy gap (Figure 1.5) (Anizaim *et al.*, 2021). The small energy gap is an excellent property for optoelectronic devices such as optical limiting, OLEDs, and solar cell materials (Zainuri *et al.*, 2018a).



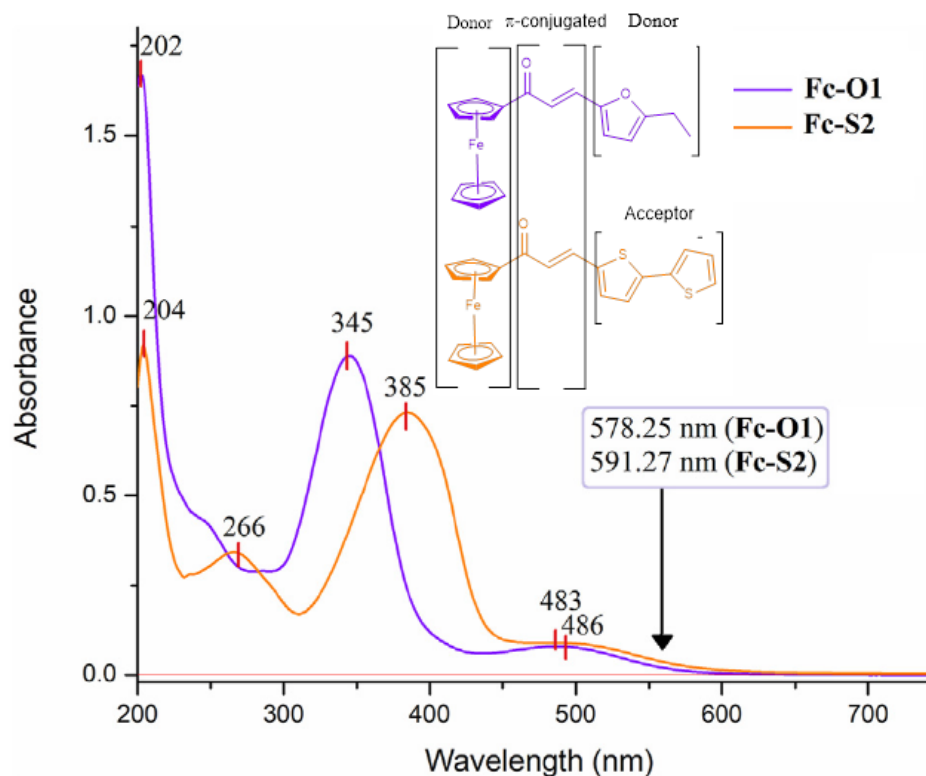


Figure 1.5 UV-Vis spectrum of D- $\pi$ -A and D- $\pi$ -D chalcone derivative (Anizaim *et al.*, 2021).

Hydrogen bonding is the intermolecular forces that exist between the molecules of the compound. The presence of hydrogen bond may exist as D—H $\cdots$ A and D—H $\cdots$  $\pi$  configurations in the chalcone unit. The strength of hydrogen bond may varies depending on the push-pull system of the compound (Tao *et al.*, 2017). As the push-pull system exists in higher amplitude, it will strengthen the hydrogen bond configuration between the molecules. The existence of hydrogen bonding in the push-pull compounds are also influenced by the nature of anchoring substituent, crystal structures and experimental surroundings (Chipanina *et al.*, 2014). The chalcone derivative in Figure 1.6a and Figure 1.6b illustrates the head-to-tail and head-to-head orientations of intermolecular interaction, respectively, in the crystal packing position. These orientations help to facilitate the charge injection process within the molecules by enhancing the electronic delocalization properties for solar cell applications.

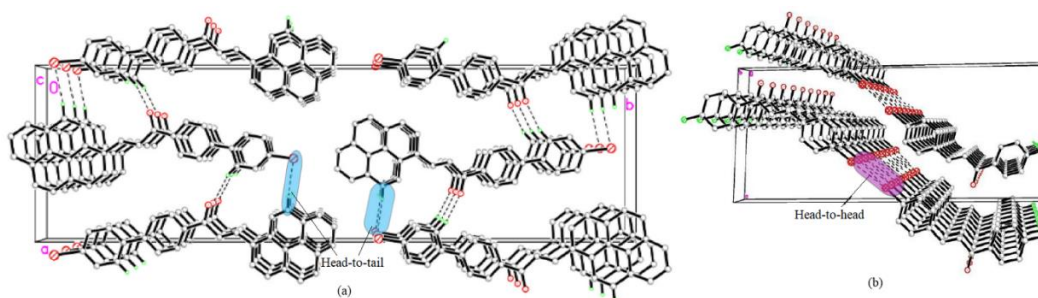


Figure 1.6 Crystal packing showing (a) head-to-tail and (b) head-to-head orientations of intermolecular interaction between the molecules (Alsaee *et al.*, 2022; Zaini *et al.*, 2018).

**PnCh** consist of a push-pull system making an excellent candidate for the photovoltaic materials (Karuppusamy *et al.*, 2017). This property fulfills the requirement for the solar cell devices to possess a good ICT. The substitution of anchoring group can be varied by adding the methoxy ( $-\text{OCH}_3$ ) and  $-\text{COOH}$  functional group which previously reported as a good anchoring property in facilitating the electron transfer (Anizaim *et al.*, 2020; Nizar *et al.*, 2021).

### 1.3 The $\pi$ -conjugated PnCh System as Dye-Sensitizer

Solar cell has been discovered since 1950s as a technology to convert sunlight into the electrical energy (Bosio *et al.*, 2020). Since its discovery, solar cell has become a promising candidate for research study developing three generations stage (Figure 1.7) throughout the time and multiple of fabrications materials. Beginning with the first (1<sup>st</sup>) generation, the application of solar cells at this phase are focusing on pure silicon crystals producing a silicon-based solar cells which successfully dominate the photovoltaic market with high efficiencies (Ahmad *et al.*, 2021). Meanwhile, the second (2<sup>nd</sup>) generation are basically about thin-film technologies that offers a lower cost than the first-generation cell. The third (3<sup>rd</sup>) generation solar cells are currently gaining much attention due to its unique property since the photogenerated charge

carrier able to flow throughout the cell without p-n junction as required by the first and second generation. In recent years, the dye-sensitized solar cell (DSSC) is a third solar cell generation which has been growing rapidly due to its ability in reaching higher efficiency, simple fabrication method and eco-friendly comparing to the conventional cells (Mozaffari *et al.*, 2015).

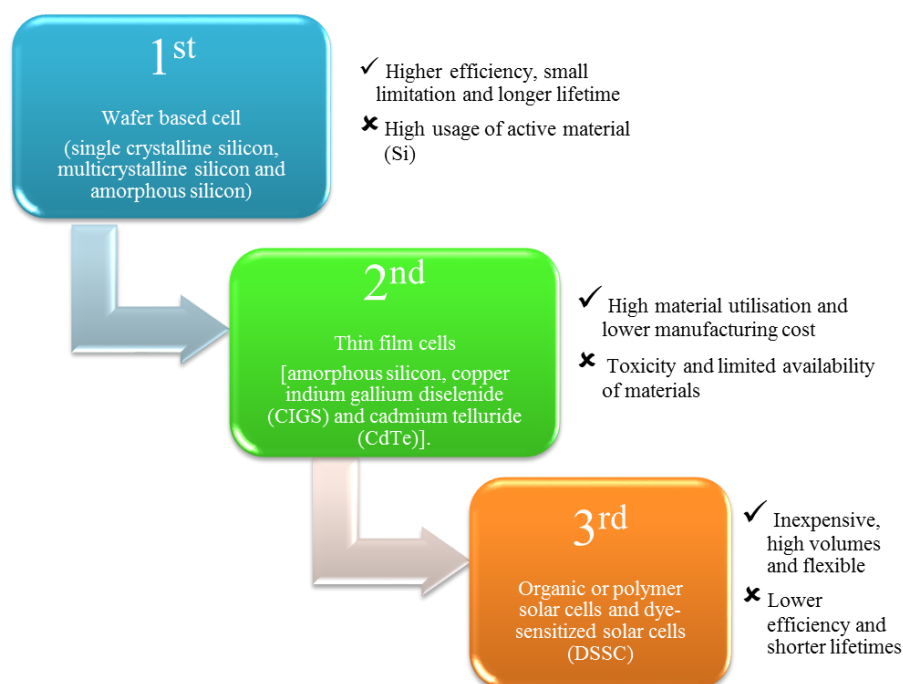


Figure 1.7 The 1<sup>st</sup>, 2<sup>nd</sup>, and 3<sup>rd</sup> generation of solar cell evolutions (Olivia-Chatelain & Barron, 2011).

Chalcone are established as the  $\pi$ -conjugated system in which widely applied in dye sensitized solar cell (DSSC) area. The conjugation between donor and acceptor group linked by  $\pi$ -conjugated configuration promotes a high photovoltaic result (Teo *et al.*, 2017). The previous research on **PnCh** derivative has reported that the composition between pyrene and chalcone become a good combination with 7.89% DSSC efficiency results (Rajakumar *et al.*, 2012). The synthesis of various anchoring group on **PnCh** as dye-sensitizer leads to the study on feasibility of electron injection

and dye regeneration. Besides, the materials of the dye-sensitizer also effect the efficiency of electron transfer as can be seen in Figure 1.8a and Figure 1.8b. The basic structure of DSSC is consist of three key parameters, particularly dye-sensitized photoanode, counter electrode and redox electrolyte (Figure 1.8).

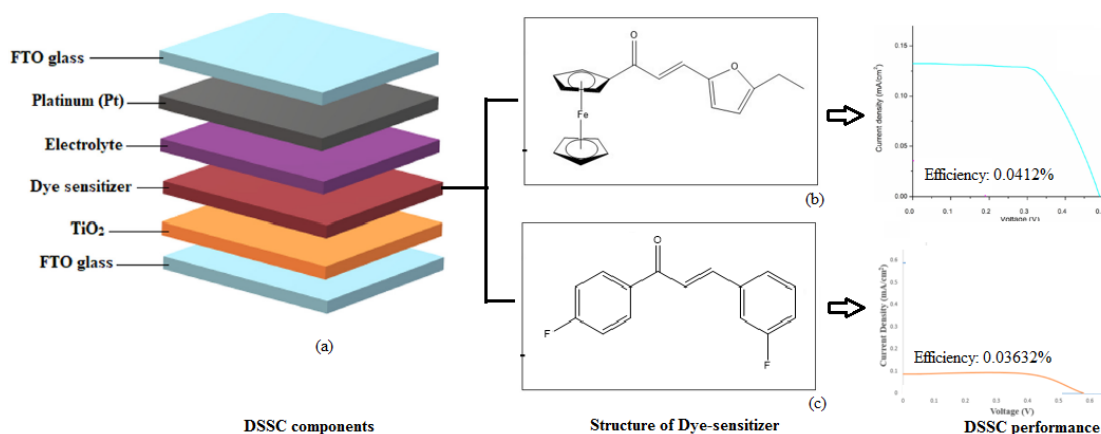


Figure 1.8 (a) The basic operation of DSSC in structure layered, DSSC performance of (b) organometallic-containing sensitizer and (c) organic-containing sensitizer (Anizaim *et al.*, 2021; Nizar *et al.*, 2021).

**PnCh** has shown the ideal characteristic of push-pull effect and efficient ICT which leads to the application of solar cells and OLEDs technology (Karuppusamy *et al.*, 2022). The previous study on **PnCh** as dye-sensitizer has shown a good conjugation between the pyrene and chalcone group due to the properties of pyrene as a potent photoreductant and the pyrene radical cation as a strong oxidant which oxidizes the iodide rapidly (Rajakumar *et al.*, 2012). Hence, a higher photocurrent and performance results are achieved with the increase in the number of pyrene-chalcone units in the redox couple of DSSC (Figure 1.9) (Rajakumar *et al.*, 2012). This feature indicates the potentiality of **PnCh** as the promising candidate in the DSSC application.

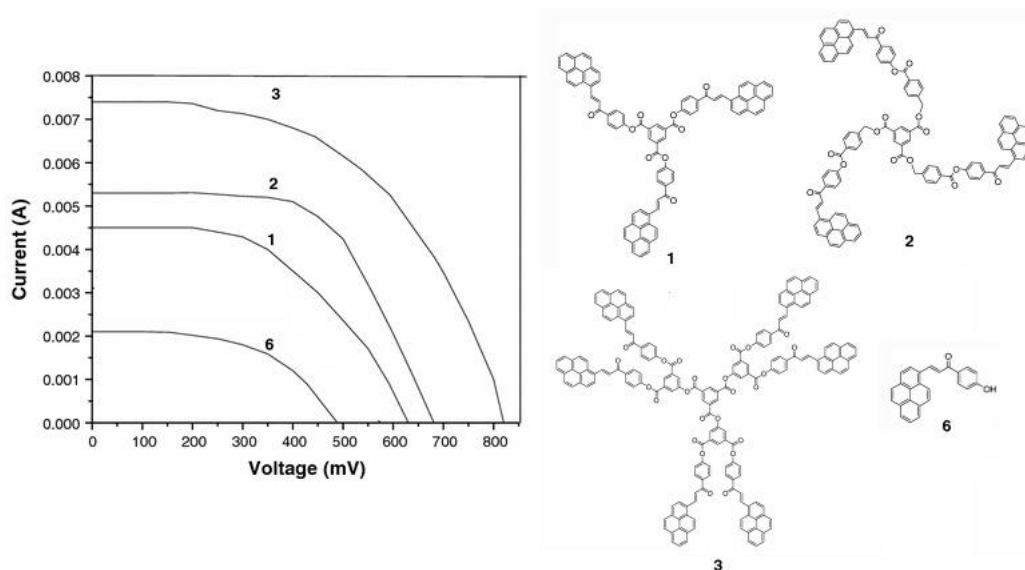


Figure 1.9 The  $J$ - $V$  curve of the previously reported compounds (Rajakumar *et al.*, 2012).

#### 1.4 Problem Statement

World's energy demand is growing fast due to the increasing population led to the consumption of human needs such as crude oil and natural gas. This situation causes several challenges concerning the reduction of fossil fuel resources, greenhouse gas emissions and environmental troubles. Being a country, in which receives sunlight throughout the year, energy production using photovoltaic technology in Malaysia is a great assist in producing potential renewable energy by converting sunlight into electrical energy. The current market marked the single-crystal silicon type solar cell has recorded more than 26% of high efficiency results, meanwhile the DSSC power conversion are stated only at 11.9% efficiency rate (Green *et al.*, 2021). These low efficiency result might be due to the weak anchoring factor of dye-sensitizer material on the  $\text{TiO}_2$  layer. The study on the best material for dye-sensitizer should be augmented to facilitate the electron transfer in DSSC, hence its conversion efficiency.

Secondly, the whole scientific community are ultimately focusing on the improvement of long-term stability of DSSC technology. According to Baxter (2012), the dye-sensitizer of DSSC is an important array for effective energy conversion. Over the period, the DSSC performance decrease with time due to the ageing of the dye-molecules (Kabir *et al.*, 2019). Besides, the appropriate position of HOMO and LUMO are required to facilitate the charge transfer for the dye regeneration process (Baxter, 2012). Consequently, the research on photophysical and photochemical properties of dye-sensitizer materials plays a significant role in extending the study on DSSC stability to meet the promises of this technology.

DSSC application have gained substantial research interest owing to the low fabrication cost comparing to the conventional solar cells. Additionally, the previous work shows that the presence of pyrene act as a strong photoreductant which increase the photocurrent in DSSCs, thus leading to the satisfaction result of solar cell efficiency (Rajakumar *et al.*, 2012). This prove that pyrene based chalcone is a potential photosensitizer in DSSCs. However, only 5 in total reported journals on pyrene based chalcone in term of DSSC technology were found (Rajakumar *et al.*, 2012; Li *et al.*, 2014a; Selvam & Subramanian, 2017; Aguilar-Castillo *et al.*, 2018; Anandkumar & Rajakumar, 2018). A huge research should be conducted in qualifying **PnCh** as dye-sensitizers of DSSC to delivers electricity in larger scale and affordable price.

## 1.5 Objectives

1. To design and synthesize the extended  $\pi$ -conjugated system of pyrenyl chalcone (**PnCh**) chromophores containing different donor or acceptor substituent groups.
2. To determine the structural and photophysical properties of the targeted **PnCh** derivatives with different substituent groups at the donor- $\pi$ -acceptor bridge.
3. To investigate the capabilities of the synthesized **PnCh** as potential dye-sensitizer.

## CHAPTER 2

### LITERATURE REVIEW

#### 2.1 The D- $\pi$ -A System of Chalcone Derivative

The D- $\pi$ -A structural chromophores consisting of donor (D) and acceptor (A) pairs which are connected to each other through a  $\pi$ -conjugated electron linkage (Khalid *et al.*, 2020). The nature of both donor and acceptor moieties plays a critical role in facilitating the ICT in D- $\pi$ -A structure compare to the D- $\pi$ -D architecture (Lu *et al.*, 2019). In the D- $\pi$ -A system, the  $\pi$ -conjugated group works as the bridge to flow the charge transfer from the donor to the acceptor group (Fitri *et al.*, 2014). According to Li *et al.*, (2014b), the degree of ICT in the push-pull system is influenced by the electronegativities and polarizabilities of the systems. Particularly, the high electropositive of donor moiety influence the polarizability of the acceptor moiety to determine the magnitude of ICT (Li *et al.*, 2014b). This D- $\pi$ -A structure facilitate the ICT between the donor and acceptor moieties and creates the push-pull configuration involving the low-energy and intense charge transfer absorption (Figure 2.1) (Kulhanek & Bures, 2012). A good flow of ICT is an important criteria since it give rise to the higher conversion efficiency in DSSC (Anizaim *et al.*, 2021).

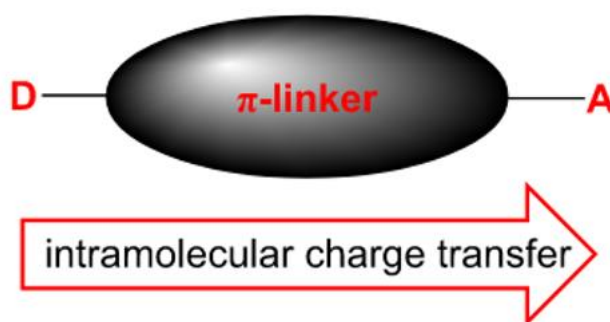


Figure 2.1 Schematic representation of D- $\pi$ -A system featuring ICT (Kulhanek & Bures, 2012).



### 2.1.1 D- $\pi$ -A configuration influence the red-shift in the absorption band

In the D- $\pi$ -A structure motif, the additional of electron-withdrawing group into the  $\pi$ -conjugated bridge has shown a bathochromic shifts in the absorption band of the UV-Vis due to the excellent flow of charge-transfer properties within the compound (Liu *et al.*, 2014). According to Karuppusamy *et al.*, (2022), the absorption maximum attributed by a series of **PnCh** has shown a longer red-shift in the absorbance spectra of the compound with D- $\pi$ -A configurations comparing to the D- $\pi$ -D structure (Figure 2.2). This is due to the anchoring of the acceptor group in the chalcone structure which further enhance the electron delocalization due to the appropriate conjugation with the pyrene moiety and  $\alpha$ ,  $\beta$ -unsaturated carbonyl group (Karuppusamy *et al.*, 2022). Hence, this further proves the chromophores with D- $\pi$ -A architecture has leads to the better energy gap results than the compound with D- $\pi$ -D configuration.

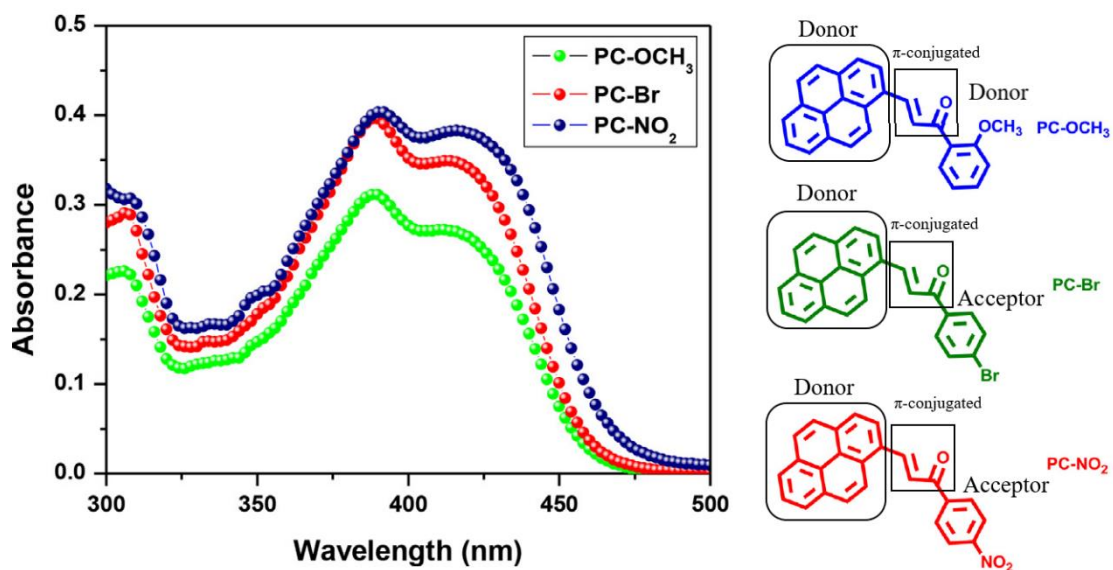


Figure 2.2 Absorption spectra of **PnCh** showing D- $\pi$ -A and D- $\pi$ -D architecture (Karuppusamy *et al.*, 2022).

### 2.1.2 Enhancement of electron injection process in D- $\pi$ -A system

The D- $\pi$ -A system of formerly reported chalcone derivative has shown an appropriate position of HOMO and LUMO energy levels from the cyclic voltammetry analysis (Figure 2.3) (Ibrahim *et al.*, 2022). The LUMO energy levels is higher than conduction band of TiO<sub>2</sub> (-4.0 eV) to ensure the electron injection process, meanwhile the HOMO energy levels is lower than redox potential of I<sup>-</sup>/I<sub>3</sub><sup>-</sup> (-4.8 eV) for the regeneration of the oxidized dye (Nizar *et al.*, 2021). The result obtained agrees with the energies of the conduction band of TiO<sub>2</sub> and the redox potential of the I<sup>-</sup>/I<sub>3</sub><sup>-</sup> electrolyte. Thus, this indicates the suitability of chalcone derivative featuring the D- $\pi$ -A system as dye-sensitizer in DSSC.

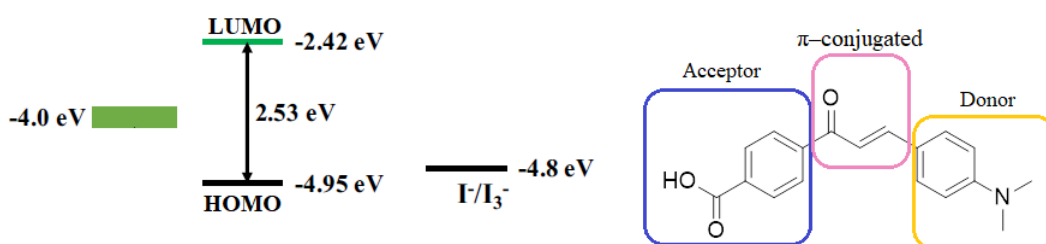


Figure 2.3 Energy level diagram of chalcone derivative with D- $\pi$ -A system (Ibrahim *et al.*, 2022).

### 2.1.3 D- $\pi$ -A configuration induce the planarity backbone

In the previous study, the D- $\pi$ -A architecture of chalcone derivative has results in the structural planarity in which the compound end-capped by the donor and acceptor group shows a planar structural in backbone (Zaini *et al.*, 2020). In comparison, a former study on chalcone derivative has reported the structure with D- $\pi$ -D configuration with twisted in structure comparing to the D- $\pi$ -A architecture (Figure 2.4) (Anizaim *et al.*, 2021). It is obtained that the substitution of acceptor group able to develop the planarity of the compound. The structural planarity plays an important role in

facilitating the ICT within the compound, thus subsequently improve the efficiency of DSSC application (So *et al.*, 2019; Anizaim *et al.*, 2021).

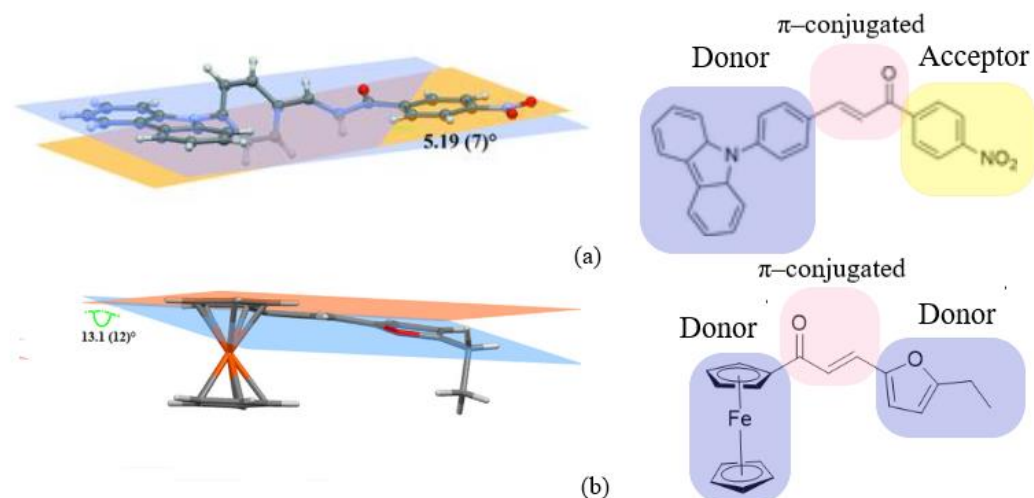


Figure 2.4 The dihedral angle between two planes for (a) D- $\pi$ -A and (b) D- $\pi$ -D architecture (Zaini *et al.*, 2020; Anizaim *et al.*, 2021).

#### 2.1.4 Improvement of DSSC efficiency in D- $\pi$ -A configuration

The former research by Nagarajan *et al.*, (2021) has shown that the conjugation of electron acceptor group able to provide the efficient charge separation and ICT throughout the compound by facilitating the photostability of the organic dyes. This study agrees with the previously reported study by Anizaim *et al.*, (2021) showing the power conversion efficiency achieve by the D- $\pi$ -A structure are higher comparing to the chalcone derivative with D- $\pi$ -D configuration (Figure 2.5). This is due to the chalcone-containing D- $\pi$ -A structure motif improve the electron transfer from the electron donor to the electron acceptor through the  $\pi$ -spacer unit more efficiently than D- $\pi$ -D structure (Fitri *et al.*, 2014).

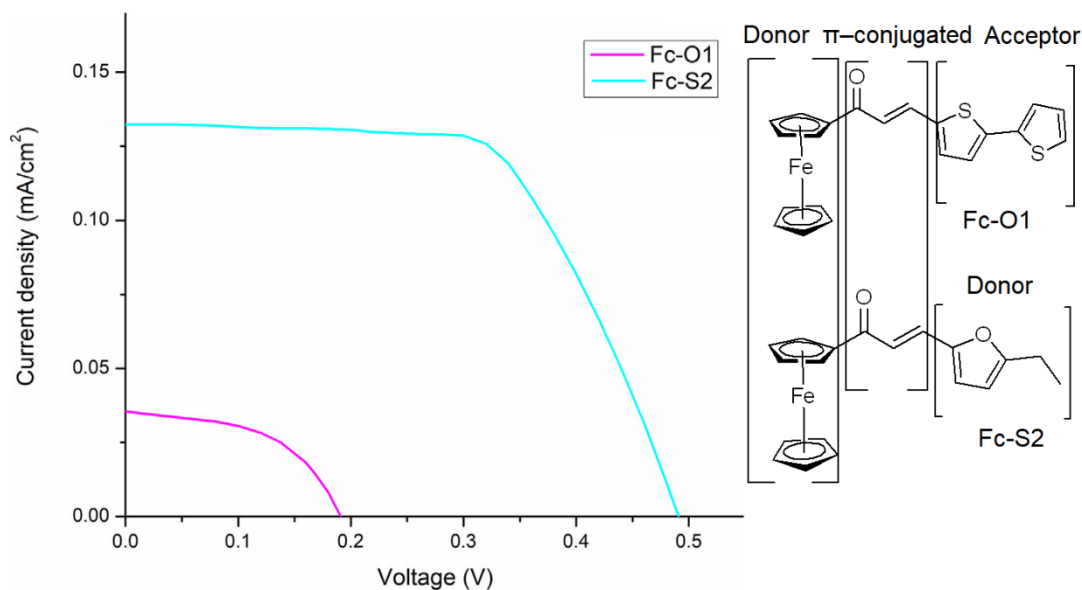


Figure 2.5 *J-V* curves for DSSCs based on D- $\pi$ -A and D- $\pi$ -D architecture (Anizaim *et al.*, 2021).

## 2.2 The Synthetic Process of Pyrenyl Chalcone (PnCh)

Chalcone derivatives are fundamentally build by the conjugation of  $\alpha$ ,  $\beta$ -unsaturated carbonyl system with two aromatic rings (Xu *et al.*, 2019). Several approaches have been deployed in the synthesis process of chalcone including Suzuki coupling reaction (Vieira *et al.*, 2012; Wang *et al.*, 2014; Duddukuri *et al.*, 2018), Wittig reaction (Kannan *et al.*, 2019; Al-Ostoot *et al.*, 2021; Jassim & Younis, 2021), Friedel-Crafts acylation with cinnamoyl chloride (More *et al.*, 2012; Zhou *et al.*, 2012; Rammohan *et al.*, 2020), Photo-Fries rearrangement of phenyl cinnamates (Sharma & Saraswat, 2021) and Claisen-Schmidt condensation (Gharib *et al.*, 2014; Kim *et al.*, 2016; Farooq & Ngaini, 2019; Nizar *et al.*, 2021). Referring to Nasir *et al.*, (2013) and Tiecco *et al.*, (2016), Claisen-Schmidt condensation method is the most promising technique that has been widely used in chalcone synthesis due to its green synthetic process and low toxicity properties.

The Claisen-Schmidt condensation (Figure 2.6) involves a simple preparation of chalcone by reacting the aldehyde and ketone (Sahu *et al.*, 2012; Farooq & Ngaini, 2019). This reaction is carried out with the aid of the base catalyst such as Ba(OH)<sub>2</sub>, LiOH, SOCl<sub>2</sub>, KOH and NaOH to speed-up the reaction activity (Patil & Bhanage, 2013; Kommidi *et al.*, 2015; Zaini, *et al.*, 2019a). The resultant yield obtained from the reaction are further recrystallized using the suitable solvent and appropriate crystallization method like slow evaporation (Indira *et al.*, 2002), vapor diffusion (Jacquemet *et al.*, 2004) and liquid-liquid diffusion (Tordo *et al.*, 2021) technique.

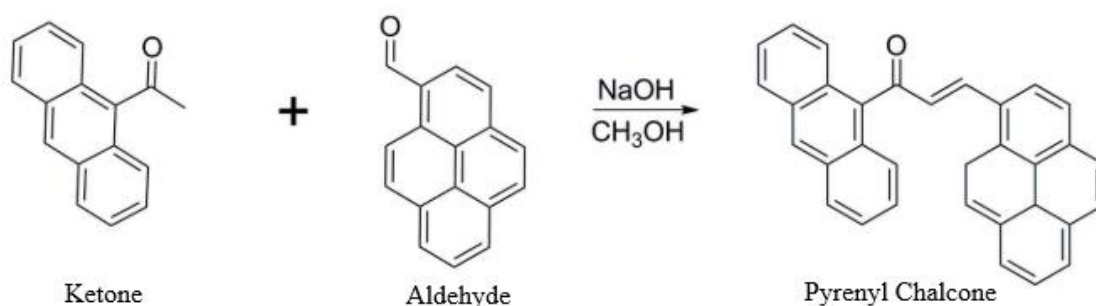


Figure 2.6 The synthesis scheme of **PnCh** derivative (Zainuri *et al.*, 2018b).

### 2.3 Fourier Transform Infrared (FTIR) Studies

FTIR is a vibrational spectroscopy study which provides the information regarding the functional group, bonding type and molecular conformation of the compounds (Talari *et al.*, 2017). Attenuated total reflection (ATR) has been used in preparing the sample for FTIR analysis due to the easier procedure comparing to the conventional potassium bromide (KBr) pellet method (Tahir *et al.*, 2017). The absorbance spectra of ATR-FTIR analysis are recorded at 600-4000 cm<sup>-1</sup> region. In chalcone derivative studies, the vibrational modes are mainly focusing on C-H stretching, C=O stretching and C=C aromatic stretching of enone bridge (Figure 2.7). Table 2.1 tabulates the previous reports of FTIR vibrational frequency for **PnCh** derivatives.

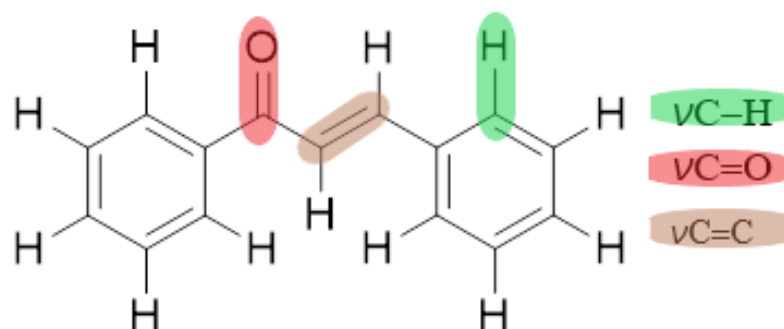


Figure 2.7 The vibrational modes studied in chalcone derivatives.

Table 2.1 Assignments of vibrational frequencies value for previously reported PnCh.

Stretching ( $\nu$ ) vibrational mode	Experimental ( $\text{cm}^{-1}$ )
$\nu\text{C-H}$	3039 (Atahan, 2021) 3056 (Sun <i>et al.</i> , 2019) 3047 (Karuppusamy <i>et al.</i> , 2019) 3041 (Karuppusamy & Kannan, 2020) 3038 (Alsaee <i>et al.</i> , 2022)
$\nu\text{C=O}$	1645 (Atahan, 2021) 1641 (Sun <i>et al.</i> , 2019) 1637–1661 (Karuppusamy & Kannan, 2018) 1662 (Karuppusamy <i>et al.</i> , 2019) 1670 (Alsaee <i>et al.</i> , 2022) 1651–1645 (Zhao <i>et al.</i> , 2017)
$\nu\text{C=C}$	1587–1588 (Karuppusamy & Kannan, 2018) 1505 (Karuppusamy <i>et al.</i> , 2019) 1584 (Karuppusamy & Kannan, 2020) 1584 (Alsaee <i>et al.</i> , 2022)

According to Prasad *et al.*, (2015), the aromatic C–H stretching bond occurs above  $3000\text{ cm}^{-1}$  frequency in weak to moderate intensity. The intensity C–H stretching vibrations are depending on the charge transfer between the hydrogen and the carbon atom (Maidur *et al.*, 2017). Besides, the vibrational frequency of C–H are not influenced by the other substituents resulting it is commonly found in the expected regions (Kumar *et al.*, 2017).

The vibration band of C=O stretching appears due to the carbonyl group with an intense peak in the infrared band (Maidur *et al.*, 2018). The C=O vibration band are expected in the range of wavenumber 1600–1700  $\text{cm}^{-1}$  as previously reported (Zainuri *et al.*, 2018a). This phenomenon are also depending on the double bond strengths, the lone pair of electrons on oxygen and the steric effects occurrence in the molecules (Zaini *et al.*, 2019b).

In previously reported study, the C=C stretching mode are expected at the wavenumber 1400–1625  $\text{cm}^{-1}$  when conjugated with the carbonyl group (C=O) (Prasad *et al.*, 2015). The vibrations of  $\nu\text{C}=\text{C}$  located at  $\alpha$ ,  $\beta$ -unsaturated double bond are related to the magnitude of charge transfer between the donor and acceptor group (Twinkle *et al.*, 2020). Figure 2.8 shows the FTIR spectrum of previously reported **PnCh** derivative (Alsaee *et al.*, 2022).

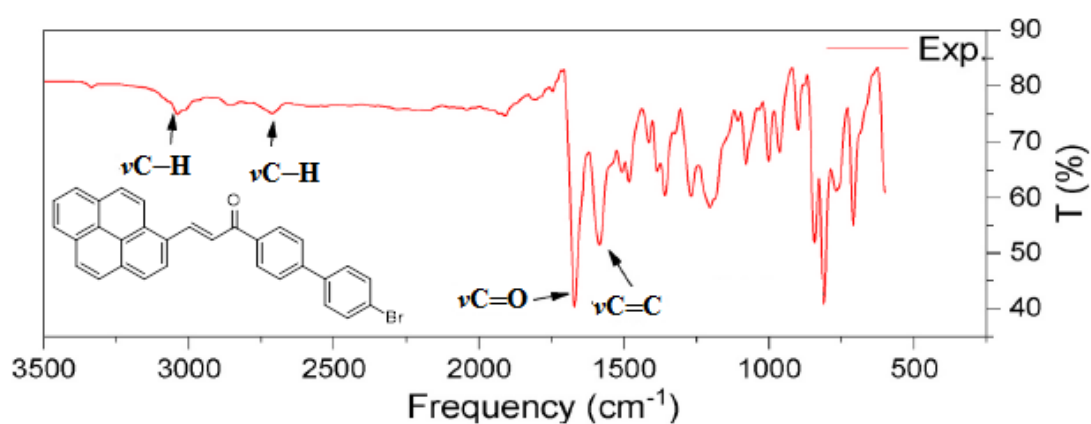


Figure 2.8 The FTIR spectrum of **PnCh** compound (Alsaee *et al.*, 2022).

## 2.4 Nuclear Magnetic Resonance (NMR) Studies

Nuclear Magnetic Resonance (NMR) is a technology conducted to clarify the molecule structure of the compound in organic chemistry field (Marccone *et al.*, 2013). The NMR studies of **PnCh** derivative are focusing on  $^1\text{H}$  and  $^{13}\text{C}$  isotropic chemical shifts at the enone bridge.

A few studies on  $^1\text{H}$  NMR analyses have been tabulated (Table 2.2) showing the ethylenic protons of enone moiety,  $\text{H}_\alpha$  and  $\text{H}_\beta$  manifest two separate doublets in the range of 7.33-7.82 ppm and 7.88-8.56 ppm, respectively. The geometric isomer of *cis* shifted more upfield due to the smaller coupling constant, meanwhile the *trans* isomer shifted more downfield on the NMR spectrum (Brizgys *et al.*, 2012; Chen *et al.*, 2014).

Table 2.2  $^1\text{H}$  isotropic chemical shifts (ppm).

Literature	$^1\text{H}$ NMR	
	$\text{H}_\alpha$	$\text{H}_\beta$
Sakthinathan <i>et al.</i> (2013)	7.33-7.57	7.88-8.13
Atahan (2021)	7.51	7.96
D'Aléo <i>et al.</i> (2015)	7.51-7.82	8.22-8.56

Atahan, (2021) reported an NMR study of **PnCh** showing the doublets appointed to  $\alpha$  and  $\beta$  protons of double bond at 7.51 and 8.36 ppm, respectively (Figure 2.9). The value of  $\text{H}_\alpha$  and  $\text{H}_\beta$  obtained for the **PnCh** in the NMR spectrum are in the expected range.

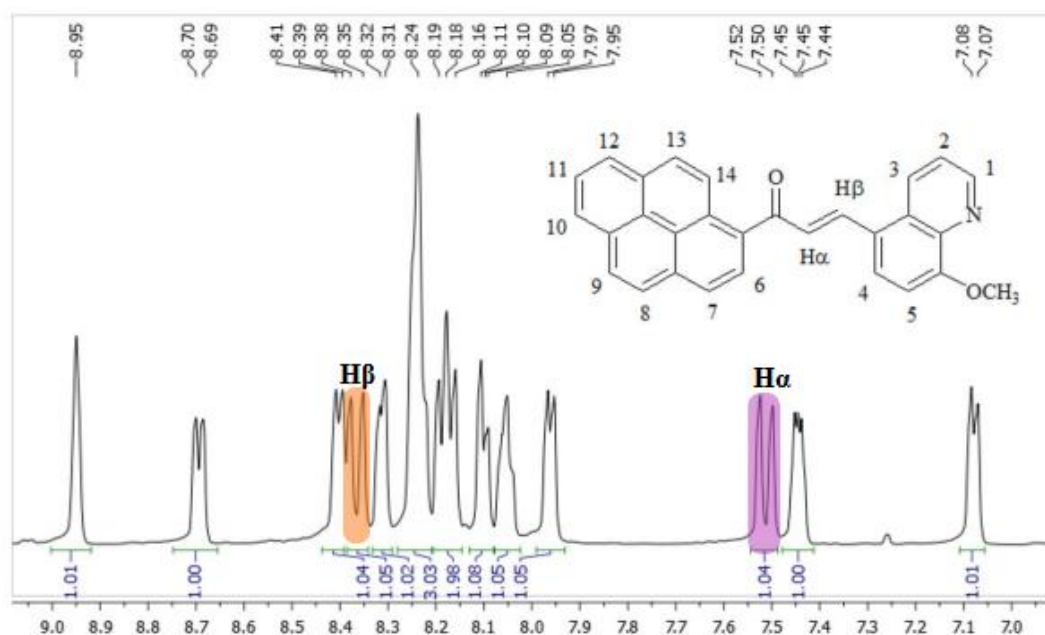


Figure 2.9 The  $^1\text{H}$  NMR spectrum of **PnCh** (Atahan, 2021).



Based on the formerly reported study, the electronegative functional group (C=O),  $C_\alpha$  and  $C_\beta$  results of  $^{13}\text{C}$  NMR are tabulated (Table 2.3). The C=O electronegative functional group polarizes the electron distribution and shifted to the most deshielded area which are 189.44-195.95 ppm. Figure 2.10 shows the  $^{13}\text{C}$  NMR spectrum of **PnCh** derivative.

Table 2.3  $^{13}\text{C}$  isotropic chemical shifts (ppm).

Literature	$^{13}\text{C}$ NMR (ppm)		
	C=O	$C_\alpha$	$C_\beta$
Sakthinathan <i>et al.</i> (2013)	194.60-195.95	124.04-123.51	144.56-145.41
Atahan (2021)	195.30	124.70	149.50
D'Aléo <i>et al.</i> (2015)	189.44-192.58	111.71-125.90	138.45-141.34

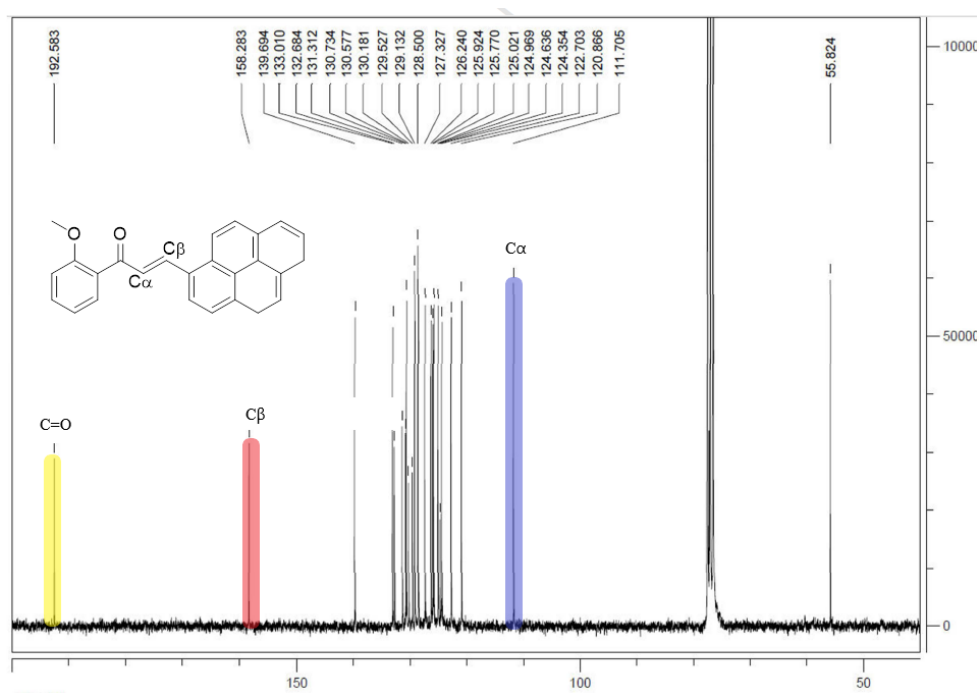


Figure 2.10 The  $^{13}\text{C}$  NMR spectrum showing C=O,  $C_\alpha$  and  $C_\beta$  in **PnCh** (D'Aléo *et al.*, 2015).

## 2.5 X-Ray Crystallography: Molecular and Crystal Packing Studies

### 2.5.1 Molecular Structure of PnCh

The molecular structure is defined as the three-dimensional arrangement of the molecules which are illustrated with the aid of SHELXTL programs (Ki *et al.*, 2017; Sheldrick, 2015). The understanding of the molecular structure is significant in studying the properties of intramolecular charge transfer (ICT) within the compound. Figure 2.11 illustrates the molecular structure for the related studies of the basic **PnCh** derivative.

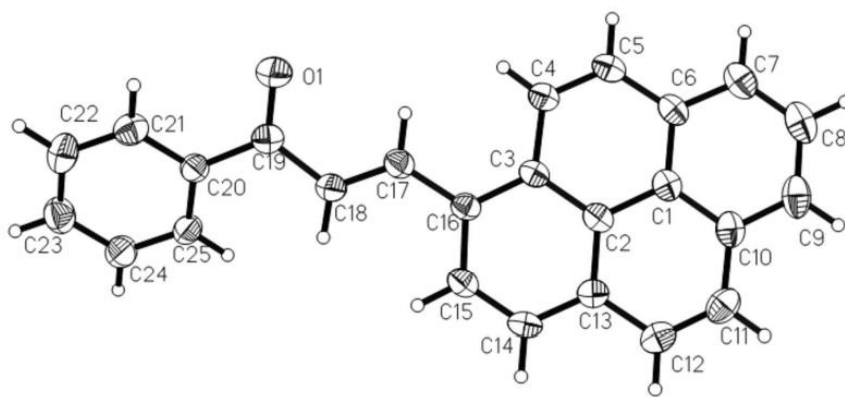


Figure 2.11 The molecular structure of core **PnCh** (Wang *et al.*, 2008).

The chalcone derivatives exist in flexible formation which can form several configurations in the molecular structure such as *cis*, *trans*, *s-cis* and *s-trans* (Figure 2.12). The *cis* and *trans* are used to differentiate the configurations of hydrogen atoms across the C=C bond (Ashenurst, 2021). Meanwhile, the *s-cis* and *s-trans* conformations are related to the rotation of the single bond linked by the two double bonds (C=O and C=C) as described by (Gunawardena, 2022).

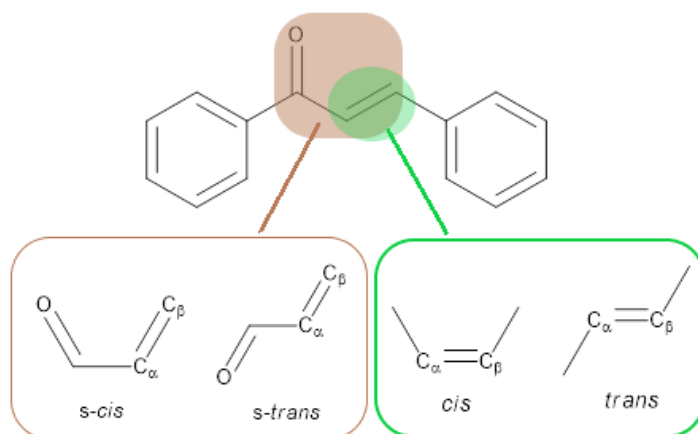


Figure 2.12 The *cis*, *trans*, *s-cis* and *s-trans* configurations in chalcone.

According to the previous research, the **PnCh** are mostly configured by *s-trans* confirmations (Sun *et al.*, 2012; Du *et al.*, 2017; Zainuri *et al.*, 2018a; Alsaee *et al.*, 2022; Wang *et al.*, 2008). Du *et al.*, (2017) reported a structure of **PnCh** with *s-trans* (O=C38 and C28=C26) configuration and *trans* (C28=C26) configuration (Figure 2.13).

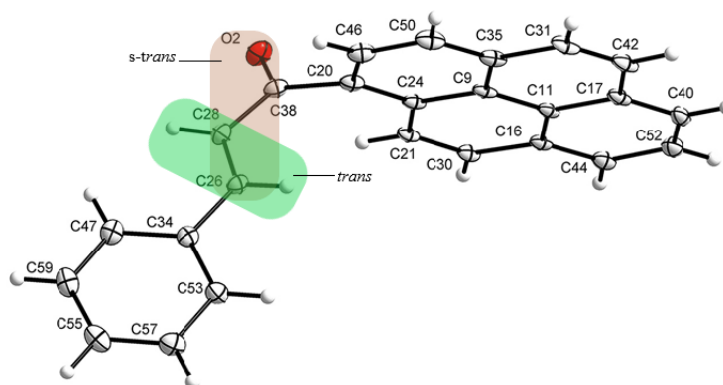


Figure 2.13 **PnCh** with *s-trans* and *trans* configurations (Du *et al.*, 2017).

Besides, the configurations of **PnCh** are also involved by *s-cis* confirmations with respect to the vinylenic double bond (C=C) and carbonyl group (C=O) as depicted in the molecular structure (Figure 2.14). Aksöz & Ertan (2011) reported that the *s-cis* conformation is the most stable conformer which may lead to the high planarity of the molecular structure (Wang *et al.*, 2008; Xu *et al.*, 2019; Alsaee *et al.*, 2022). The

planarity of the structure contributes to the good flow of ICT which is the important features in the applications of DSSC (Anizaim *et al.*, 2021).

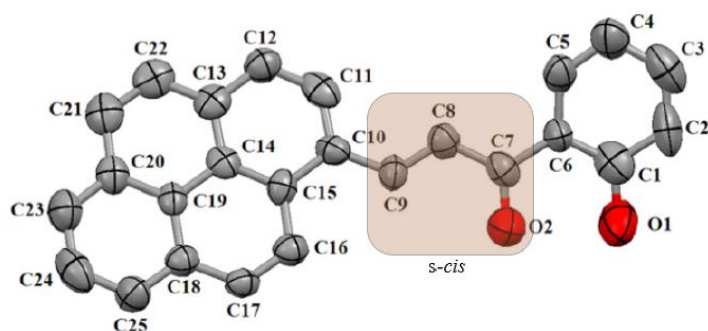


Figure 2.14 The *s-cis* configuration of **PnCh** (Sun *et al.*, 2012).

The molecular structure of **PnCh** manifest the small dihedral angle which represents the planar configuration and good charge transfer properties (Alsaee *et al.*, 2022). According to Anizaim *et al.*, (2021), the compound with high molecular planarity leads to a good flow of ICT. As can be seen in Figure 2.15, D'Aléo *et al.*, (2015) has reported two **PnCh** consist of small dihedral angle between pyrene unit and aromatic ring at  $9.59^\circ$  and  $20.09^\circ$  for compounds without and with methoxy substituents (-OMe), respectively. Hence, it is obtained that the presence of certain substituents such as methoxy group able to increase planarity in the compound, thus facilitate the ICT throughout the molecule (Che & Perepichka, 2020).

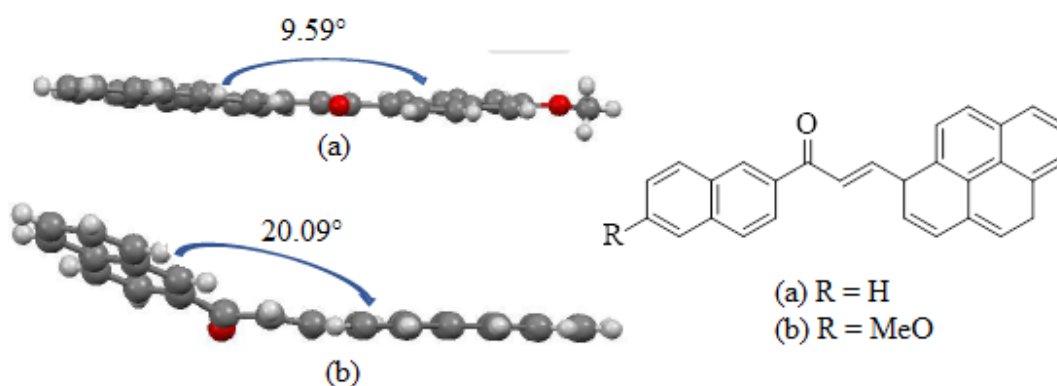


Figure 2.15 The small dihedral angle of **PnCh** (a) without and (b) with the presence of methoxy substituents (Che & Perepichka, 2020).